Eur. Phys. J. E (2015) **38**: 43
DOI 10.1140/epje/i2015-15043-2

THE EUROPEAN PHYSICAL JOURNAL E

Regular Article

High-frequency vibration effect on the stability of a horizontal layer of ternary fluid*

Tatyana Lyubimova[1,2,a]

[1] Institute of Continuous Media Mechanics UB RAS, 1, Koroleva Str., 614013, Perm, Russia
[2] Perm State University, 15, Bukireva St., 614990, Perm, Russia

Received 15 July 2014
Published online: 25 May 2015 –

Abstract. The effect of small-amplitude high-frequency longitudinal vibrations on the stability of a horizontal layer of ternary fluid is studied in the framework of average approach. Long-wave instability is studied analytically and instability to the perturbations with finite wave numbers is studied numerically. It is found that, similar to the case when vibrations are absent, for ternary fluids there exist monotonic and oscillatory long-wave instability modes. The calculations show that the vibrations lead to destabilization in the case of heating from below and to stabilization in the case of heating from above. Additionally, vibrations influence on the parameter range where long-wave instability is most dangerous. New, vibrational, instability modes are found which leads to the existence of convection in zero-gravity conditions.

1 Introduction

It is known that vibrations are able to make significant effect on a stability of equilibrium states and to create new equilibrium states. The simplest example of this is the Kapitza pendulum. It was found that vertical high-frequency vibrations of the suspension point can stabilize the state with the inverted bob position, *i.e.* the state with the bob above the point of suspension and horizontal high frequency vibrations of the suspension point create new stable equilibrium states with the inclined position of the pendulum [1, 2]. Similar effects were observed for hydrodynamical systems in [3]: vertical high-frequency vibrations were able to stabilize the equilibrium state of a two-layer system subjected to gravity in which a denser fluid is located above a less dense one, preventing the development of the Rayleigh-Taylor instability and horizontal high-frequency vibrations created a new stable equilibrium states with an inclined fluid interface.

As shown for the first time in [4], vibrations can generate time-average flows even in the absence of other mechanisms inducing flows. The comprehensive review of works on this phenomenon called thermal vibrational convection can be found in [5]. The effect of small-amplitude high-frequency vibrations of different orientations on the onset of the Soret-driven convection in a horizontal layer of binary fluid was studied theoretically, in the framework of average approach in [6, 7]. Stability boundaries to monotonic long-wave perturbations and monotonic and oscillatory short-wave perturbations are obtained. In [8] experimental investigation of the effect of controlled vibrations on the diffusion and thermodiffusion processes in water-ethanol binary mixtures of different concentrations in microgravity conditions was performed using the SODI (Selectable Optical Diagnostics Instrument) instrument on board the International Space Station. The preparation of this experiment and the first experimental results are discussed in [9–14].

The behaviour of multicomponent fluids is more complex. As shown in [15], in the case of horizontal layer of multicomponent fluid, additionally to the monotonic long-wave instability there exists an oscillatory long-wave instability mode. The goal of the present paper is to study the effect of small-amplitude high-frequency vibrations on the onset of the Soret-driven convection in a horizontal layer of ternary fluid.

2 Problem formulation. Governing equations

Let us consider Soret-driven convection of multicomponent fluid in a horizontal layer subjected to gravity field and vertical temperature gradient. We assume that the density of the mixture is linear function of temperature and component concentrations:

$$\rho = \rho_0(1 - \beta_T(T - T_0) - \boldsymbol{I} \cdot B(\boldsymbol{C} - \boldsymbol{C}_0)). \qquad (1)$$

Here T is the temperature, $\boldsymbol{C} = (C_1, \ldots, C_{n-1})^T$ is the vector of concentrations, ρ_0, $\boldsymbol{C}_0$ and T_0 are the refer-

* Contribution to the Topical Issue "Thermal non-equilibrium phenomena in multi-component fluids" edited by Fabrizio Croccolo and Henri Bataller.

[a] e-mail: lubimova@psu.ru

ence density, vector of concentrations and temperature of the mixture respectively, $\beta_T = -\frac{1}{\rho_0}\frac{\partial\rho}{\partial T}\big|_{C_i,i=1,\ldots,n-1}$ is the thermal expansion coefficient, $B = \mathrm{diag}\{\beta_{C_1},\ldots,\beta_{C_{n-1}}\}$ is the diagonal matrix of solutal expansion coefficients $\beta_{C_i} = -\frac{1}{\rho_0}\frac{\partial\rho}{\partial C_i}\big|_{T,C_j,j=1,\ldots,n-1,j\neq i}$, $\boldsymbol{I} = (1,\ldots,1)$.

Equations for the Soret-driven convection of multicomponent mixture in an effective gravity field consisting of the gravitational and vibrational fields in Boussinesq approximation are

$$\frac{\partial\mathbf{v}}{\partial t} + \mathbf{v}\cdot\nabla\mathbf{v} = -\frac{1}{\rho}\nabla p + \nu\nabla^2\mathbf{v} - \mathbf{g_e}\left[\beta_T(T-T_0) + \boldsymbol{I}\cdot B(\boldsymbol{C}-\boldsymbol{C}_0)\right], \quad (2)$$

$$\frac{\partial T}{\partial t} + \mathbf{v}\cdot\nabla T = \chi\nabla^2 T, \quad (3)$$

$$\frac{\partial \boldsymbol{C}}{\partial t} + \mathbf{v}\cdot\nabla\boldsymbol{C} = D\nabla^2\boldsymbol{C} + \boldsymbol{D}_T\nabla^2 T, \quad (4)$$

$$\nabla\cdot\mathbf{v} = 0, \qquad \mathbf{g_e} = \mathbf{g} - a\omega^2\ddot{f}(\tau)\mathbf{n}. \quad (5)$$

Here $\mathbf{g}$ is the gravitational acceleration, ν is the mixture viscosity, D is the molecular diffusion coefficient matrix, $\boldsymbol{D}_T$ is the vector of thermal diffusion coefficients, $\tau = \omega t$, the function $f(\tau)$ is normalized by the condition $\overline{\dot{f}^2} = 1/2$, the other notations are conventional.

The cross diffusion terms in eqs. (2)-(5) can be eliminated by diagonalizing the molecular diffusion coefficient matrix, which reduces the number of governing parameters. Such transformation can be written as [16]

$$\boldsymbol{C} = MQ^{-1}\hat{\boldsymbol{C}}, \qquad \boldsymbol{D}_T = MQ^{-1}\hat{\boldsymbol{D}}_T, \quad (6)$$

where M is a matrix whose columns are the eigenvectors $m_i = (m_{i,1},\ldots,m_{i,n-1})^T$ of the diffusion matrix D; $Q = \mathrm{diag}\{q_1,\ldots,q_{n-1}\}$, $q_i = \beta_{C_i}^{-1}\sum_{j=1}^{n-1}\beta_{C_j}m_{ij}$.

Applying transformations (6) to the state equation, we obtain

$$\rho(T,\hat{\boldsymbol{C}}) = \rho_0(1-\beta_T(T-T_0) - \boldsymbol{I}\cdot B(\hat{\boldsymbol{C}}-\hat{\boldsymbol{C}}_0)) \quad (7)$$

and eqs. (2)-(5) are transformed to

$$\frac{\partial\mathbf{v}}{\partial t} + \mathbf{v}\cdot\nabla\mathbf{v} = -\frac{1}{\rho}\nabla p + \nu\nabla^2\mathbf{v} - \mathbf{g_e}\left[\beta_T(T-T_0) + \boldsymbol{I}\cdot B(\hat{\boldsymbol{C}}-\hat{\boldsymbol{C}}_0)\right], \quad (8)$$

$$\frac{\partial T}{\partial t} + \mathbf{v}\cdot\nabla T = \chi\nabla^2 T, \quad (9)$$

$$\frac{\partial \hat{\boldsymbol{C}}}{\partial t} + \mathbf{v}\cdot\nabla\hat{\boldsymbol{C}} = \hat{D}\nabla^2\hat{\boldsymbol{C}} + \hat{\boldsymbol{D}}_T\nabla^2 T, \quad (10)$$

$$\nabla\cdot\mathbf{v} = 0. \quad (11)$$

Here $\hat{D}$, $\hat{\boldsymbol{D}}_T$ are new molecular diffusion and thermal diffusion coefficients respectively.

We consider the effect of small-amplitude high-frequency vibrations. Namely, the vibration amplitude is assumed to be small as compared to the ratio of the characteristic size to the Boussinesq parameter:

$$a \ll \left\{\frac{L}{\beta_T\Delta T}, \frac{L}{\beta_{C_i}\Delta C_i}\right\} \quad (12)$$

and the vibration period is assumed to be small in comparison with all hydrodynamical time scales:

$$T \ll \left\{\frac{L^2}{\nu}, \frac{L^2}{\chi}, \frac{L^2}{D_{ij}}\right\}. \quad (13)$$

At the same time vibrations are considered as non-acoustic $L/c \ll T$, *i.e.* compressibility effects are neglected. Here L is the characteristic size, c is the sound velocity.

If the restrictions (12) and (13) are satisfied, it is convenient to decompose all hydrodynamical fields into the sums of slowly varying (average) and quickly oscillating (pulsational) components and to obtain equations for the pulsational and average components by introducing hierarchy of time scales and applying multiple-scale method [17]. Restrictions (12) and (13) allow to neglect non-linear and viscous terms in the equations for pulsational fields.

Equations for the Soret-driven convection of multicomponent fluid subjected to the gravity field and high-frequency small-amplitude vibrations obtained in the way described above in the dimensionless form are:

$$\frac{\partial\boldsymbol{u}}{\partial t} + \boldsymbol{u}\cdot\nabla\boldsymbol{u} = -\nabla p + \nabla^2\boldsymbol{u} + \mathrm{Pr}^{-1}\,\mathrm{Ra}(T + \boldsymbol{I}\cdot\boldsymbol{C})\boldsymbol{e} + \mathrm{Pr}^{-1}\,\mathrm{Ra_v}\,(\boldsymbol{V}\cdot\nabla)\left[(T+\boldsymbol{I}\cdot\boldsymbol{C})\boldsymbol{n} - \boldsymbol{V}\right], \quad (14)$$

$$\frac{\partial T}{\partial t} + \boldsymbol{u}\cdot\nabla T = \mathrm{Pr}^{-1}\nabla^2 T, \quad (15)$$

$$\frac{\partial\boldsymbol{C}}{\partial t} + \boldsymbol{u}\cdot\nabla\boldsymbol{C} = SC\left(\nabla^2\boldsymbol{C} - \boldsymbol{\psi}\nabla^2 T\right), \quad (16)$$

$$\mathrm{div}\,\boldsymbol{u} = 0, \qquad \mathrm{div}\,\boldsymbol{V} = 0, \qquad \mathrm{curl}\,\boldsymbol{V} = \nabla(T + \boldsymbol{I}\cdot\boldsymbol{C})\times\boldsymbol{n}. \quad (17)$$

Here $\boldsymbol{u}$, T and $\boldsymbol{C}$ are average velocity, temperature and vector of concentrations, $\boldsymbol{V}$ is the pulsational velocity amplitude, $\boldsymbol{e}$ is the unit vector directed vertically upward, $\boldsymbol{n}$ is the unit vector in the direction of vibrations. Further below the hat for the transformed variable $\boldsymbol{C}$ is omitted. Equations are written in the dimensionless form. The following quantities are introduced as the scales: L for the length, ν/L for the velocity, L^2/ν for the time, $\rho_0\nu^2/L^2$ for the pressure, ΔT for the temperature, $\beta_T\Delta T B^{-1}$ for the concentration, $\beta_T\Delta T$ for the pulsational velocity amplitude; the same notations are kept for the dimensionless variables.

Equations (14)-(17) contain the following dimensionless parameters: $\boldsymbol{\psi} = -\beta_T^{-1}B\hat{D}^{-1}\hat{\boldsymbol{D}}_T$ is the vector of separation ratios having the dimension $n-1$, $\mathrm{Pr} = \nu/\chi$ is the Prandtl number, $\mathrm{Ra} = \mathrm{g}\beta_T\Delta T L^3/(\nu\chi)$ is the Rayleigh number, $\mathrm{Ra_v} = (a\omega\beta_T\Delta T L)^2/(2\nu\chi)$ is the vibrational Rayleigh number and $SC = \nu^{-1}B\hat{D}B^{-1}$, $\{SC\}_{ij} = \frac{\beta_{C_i}}{\beta_{C_j}}\mathrm{Sc}_{ij}^{-1}$, $i,j = 1,\ldots,n-1$, where $\mathrm{Sc}_{ij} = \nu/\hat{D}_{ij}$ are the Schmidt numbers.

Let us consider a Soret-driven convection of multicomponent fluid in an infinite horizontal layer bounded by two parallel rigid plates $z = 0$ and $z = L$ maintained

at constant different temperatures $T = \pm\Delta T/2$ (the case $\Delta T > 0$ (Ra > 0) corresponds to the heating from below and the case $\Delta T < 0$ (Ra < 0) to the heating from above). The axis x of the Cartesian coordinate system is directed along the layer and the axis z is perpendicular to the boundaries. The layer is subjected to the gravity field and high-frequency small-amplitude vibrations in the direction of the x-axis.

Equations (14)-(17) should be completed with boundary conditions. For the problem under consideration these conditions in the dimensionless form are

$$z = 0, 1 : \boldsymbol{u} = 0, \qquad T = \pm 1/2,$$
$$\frac{\partial \boldsymbol{C}}{\partial z} - \boldsymbol{\psi}\frac{\partial T}{\partial z} = 0, \qquad V_z = 0. \tag{18}$$

The problem (14)-(18) has a solution which corresponds to the quasi-equilibrium state with zero average velocity:

$$\boldsymbol{u}_0 = 0, \qquad T_0 = T_0(z), \qquad \boldsymbol{C}_0 = \boldsymbol{C}_0(z),$$
$$V_{0x} = V_0(z), \qquad V_{0y} = 0, \qquad V_{0z} = 0. \tag{19}$$

3 Linear stability problem

Let us consider the stability of quasi-equilibrium states to small plane perturbations. Linearizing the equations with respect to small perturbations, eliminating the perturbations of pressure and horizontal components of the velocity and introducing the normal-mode perturbations

$$(u_z', T', \boldsymbol{C}', V_z') =$$
$$[w(z), \vartheta(z), \boldsymbol{\xi}(z), W(z)] \exp(-\lambda t + ikx), \tag{20}$$

and introducing the new variables by the relations $\boldsymbol{\eta} = \boldsymbol{\xi} - \boldsymbol{\psi}\vartheta$ and $W = ik\tilde{W}$, we obtain the equations for w, ϑ, $\boldsymbol{\eta}$, $\tilde{W}$ in the form

$$-\lambda\nabla^2 w = \nabla^4 w - \mathrm{Pr}^{-1}k^2\left(\mathrm{Ra} + (1+\Psi)\,\mathrm{Ra_v}\right) \times \left((1+\Psi)\vartheta + \boldsymbol{I}\cdot\boldsymbol{\eta}\right) - \mathrm{Pr}^{-1}k^2(1+\Psi)\,\mathrm{Ra_v}\,\tilde{W}', \tag{21}$$
$$-\lambda\vartheta = \mathrm{Pr}^{-1}\nabla^2\vartheta + w, \tag{22}$$
$$-\lambda\left(\boldsymbol{\eta} + \boldsymbol{\psi}\vartheta\right) = SC\,\nabla^2\boldsymbol{\eta} + \boldsymbol{\psi}w, \tag{23}$$
$$\nabla^2\tilde{W} = -\left[(1+\Psi)\vartheta' + \boldsymbol{I}\cdot\boldsymbol{\eta}'\right], \tag{24}$$

where $\nabla^2 = \partial_{zz} - k^2$, prime stands for ∂_z, $\Psi = \psi_1 + \ldots + \psi_{n-1}$.

The boundary conditions for perturbations are

$$z = 0, 1 : \quad w = w' = \tilde{W} = \vartheta = \boldsymbol{\eta}' = 0. \tag{25}$$

4 Long-wave instability

We consider the case of ternary mixture. The linear stability of quasi-equilibrium states to the long-wave perturbations was studied analytically by the expansion of all hydrodynamical fields and Rayleigh numbers into the power series with respect to the wave number:

$$(w, \vartheta, \boldsymbol{\eta}, \tilde{W}, \mathrm{Ra}, \mathrm{Ra_v}, \omega) = \sum_{n=0}^{\infty}(w_n, \vartheta_n, \boldsymbol{\eta}_n, \tilde{W}_n, \mathrm{Ra}_n, \mathrm{Ra}_{vn}, \omega_n)\,k^{2n}. \tag{26}$$

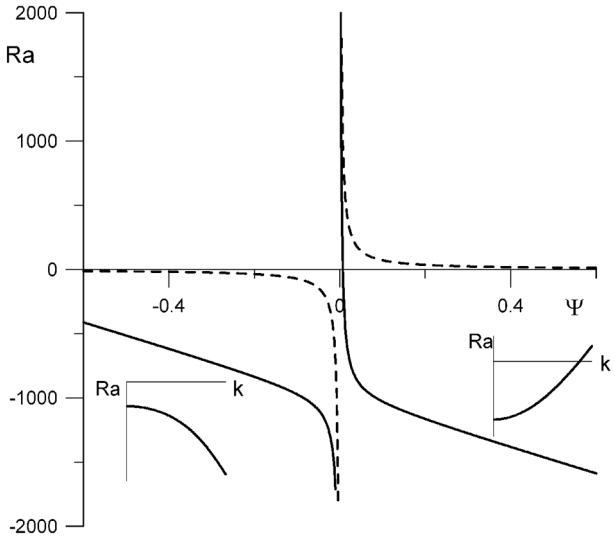

Fig. 1. Long-wave instability boundaries for $\psi_1 = 0$: solid lines $\mathrm{Ra_v} = 1000$, dashed line $\mathrm{Ra_v} = 0$; the form of the neutral curves for $\mathrm{Ra_v} = 1000$ is shown qualitatively in the fragments.

It is found that, as well as in the case when vibrations are absent (see [15]), two long-wave instability modes exist: monotonic and oscillatory. The formulas for monotonic and oscillatory instability boundaries and for the frequency of critical perturbations obtained from the solvability conditions of the first order of expansion are as follows:

$$\mathrm{Ra}_m + (1+\Psi)\,\mathrm{Ra}_{vm} = \frac{720\mathrm{Pr}}{\psi_1\,\mathrm{Sc}_1 + \psi_2\,\mathrm{Sc}_2}, \tag{27}$$
$$\mathrm{Ra}_{os} + (1+\Psi)\,\mathrm{Ra}_{vos} = \frac{720\mathrm{Pr}\,(\mathrm{Sc}_1 + \mathrm{Sc}_2)}{\mathrm{Sc}_1\,\mathrm{Sc}_2\,\Psi}, \tag{28}$$
$$\omega^2 = -\frac{\psi_1\,\mathrm{Sc}_1^2 + \psi_2\,\mathrm{Sc}_2^2}{\Psi\,\mathrm{Sc}_1^2\,\mathrm{Sc}_2^2}. \tag{29}$$

At $\mathrm{Ra_v} = 0$ the formulas (27)-(29) are reduced to the formulas obtained in [15] for the long-wave instability boundaries for ternary fluid in the absence of vibrations and at $\psi_1 = 0$ or $\psi_2 = 0$ to the formulas obtained in [6] for the long-wave monotonic instability boundary for binary fluid subjected to the high-frequency small-amplitude longitudinal vibrations (the oscillatory instability mode does not exist for the case considered in [6]).

Long-wave instability boundaries for $\psi_1 = 0$ (binary fluid) are presented in fig. 1. In the absence of vibrations, the monotonic long-wave instability boundary consists of two branches: the first branch corresponds to the heating from below (the instability domain is located above the curve) and the second branch to the heating from above (the instability domain is located below the curve). The

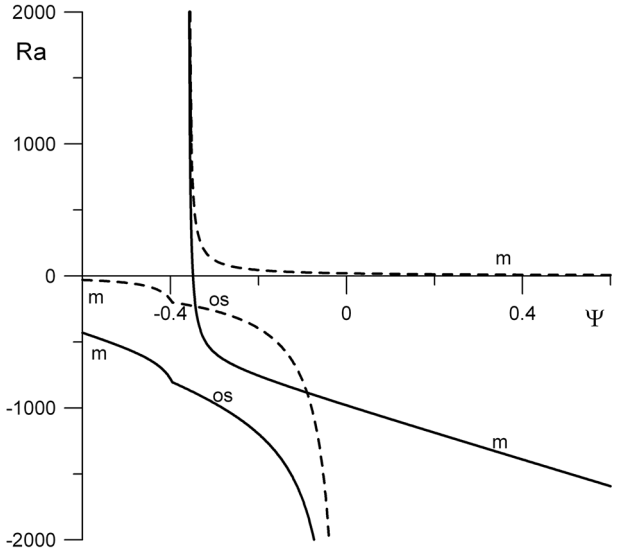

Fig. 2. Long-wave instability boundaries for $\psi_1 = -0.4$: solid lines $\mathrm{Ra_v} = 1000$, dashed line $\mathrm{Ra_v} = 0$.

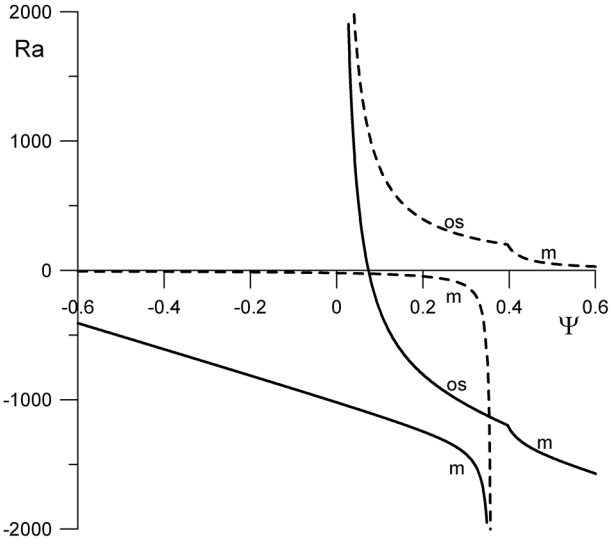

Fig. 3. Long-wave instability boundaries for $\psi_1 = 0.4$: solid lines $\mathrm{Ra_v} = 1000$, dashed line $\mathrm{Ra_v} = 0$.

oscillatory long-wave instability does not exist for binary fluids ($\omega^2 < 0$ if $\psi_1 = 0$ or $\psi_2 = 0$).

It follows from (29) that the vibrations do not change the frequency of critical perturbations (to leading order), therefore, similar to the case when the vibrations are absent, in the presence of vibrations the long-wave oscillatory instability does not exist for $\psi_1 = 0$. The monotonic long-wave instability boundaries, as one sees from fig. 1, are shifted downwards under vibrations. Thus, taking into account the location of instability domains, we may conclude that the vibrations make a destabilizing effect on the monotonic long-wave instability branch which corresponds to the heating from below and a stabilizing effect on monotonic long-wave instability branch which corresponds to the heating from above. A destabilizing effect of vibrations on the first branch leads to the existence of a monotonic long-wave instability at $\mathrm{Ra} = 0$.

Figure 2 shows the long-wave instability boundaries for ternary fluids with $\psi_1 = -0.4$. In this case, in the absence of vibrations, the monotonic long-wave instability exists at $\Psi > -0.36$ in the case of heating from below and at $\Psi < -0.36$ in the case of heating from above. For heating from above, additionally to the monotonic long-wave instability there exists the oscillatory long-wave instability. At $-0.396 < \Psi < 0$ this instability mode is the most dangerous at $\mathrm{Ra} < 0$. Vibrations make destabilizing effect on monotonic long-wave instability branch which corresponds to the heating from below and stabilizing effect on both monotonic and oscillatory long-wave instability branches which corresponds to the heating from above. As well as in the case $\psi_1 = 0$, destabilizing effect of vibrations on monotonic long-wave instability branch which corresponds to the heating from below leads to the existence of monotonic long-wave instability at $\mathrm{Ra} = 0$.

Figure 3 shows the long-wave instability boundaries for ternary fluids with $\psi_1 = 0.4$. In this case, in the absence of vibrations, the monotonic long-wave instability exists at $\Psi > 0.36$ for heating from below and at $\Psi < 0.36$ for heating from above. For heating from below, additionally to the monotonic long-wave instability there exists the oscillatory long-wave instability. At $0 < \Psi < 0.396$ this instability mode is the most dangerous at $\mathrm{Ra} > 0$. The destabilizing effect of vibrations on this mode results in the existence of oscillatory long-wave instability at $\mathrm{Ra} = 0$.

5 Instability to the perturbations with finite wave numbers. Full linear stability maps

The instability boundaries to the perturbations with finite wave numbers were obtained numerically by the shooting method [18]. Additionally, by the analysis of the second order of expansion with respect to k^2, the parameter ranges where long-wave perturbations are most dangerous were identified.

Full stability maps in the parameter plane Ψ-Ra for the binary fluid with $\mathrm{Pr} = 10$, $\mathrm{Sc_1} = 100$, $\mathrm{Sc_2} = 1000$, $\psi_1 = 0$ at $\mathrm{Ra_v} = 0$ and $\mathrm{Ra_v} = 1000$ are presented in fig. 4. As one can see, in the absence of vibrations (fig. 4, dashed lines) the long-wave monotonic instability mode remains the most dangerous at positive net separation ratios larger than 0.04; in the range $0 < \Psi < 0.04$ the monotonic perturbations with finite wave numbers are responsible for the instability and at $\Psi < 0$, $\mathrm{Ra} > 0$ the oscillatory perturbations with finite wave numbers. At $\Psi < 0$, $\mathrm{Ra} < 0$ the monotonic long-wave instability remains the most dangerous at any Ψ (in the considered parameter range).

Vibration effect on the short-wave instability is similar to that on the long-wave instability: it is stabilizing in the case of heating from above and destabiliting in the case of heating from below. Additionally, vibrations change the parameter range where the monotonic long-wave instability is most dangerous.

Vibration effect on the long-wave and short-wave monotonic and oscillatory instability modes for ternary

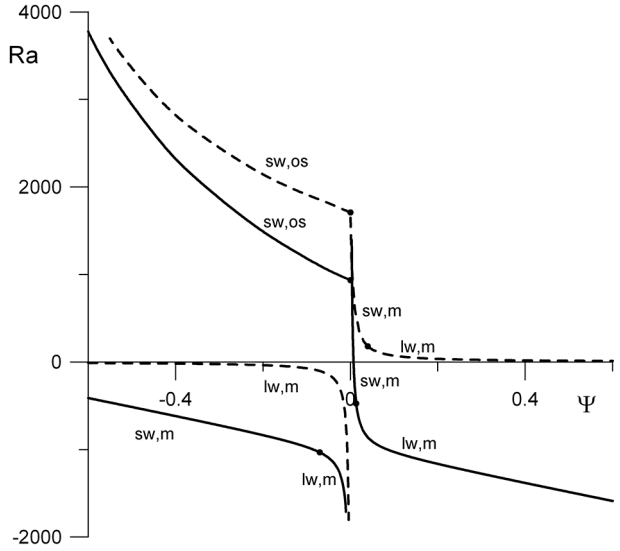

Fig. 4. Full stability map in the parameter plane Ψ-Ra for $\psi_1 = 0$: solid lines $\mathrm{Ra_v} = 1000$, dashed line $\mathrm{Ra_v} = 0$; notations near the boundaries are: lw, m long-wave monotonic instability, sw, m: short-wave monotonic instability, lw, os: long-wave oscillatory instability, sw, os short-wave oscillatory instability. The points where the instability mode changes are marked by filled circles.

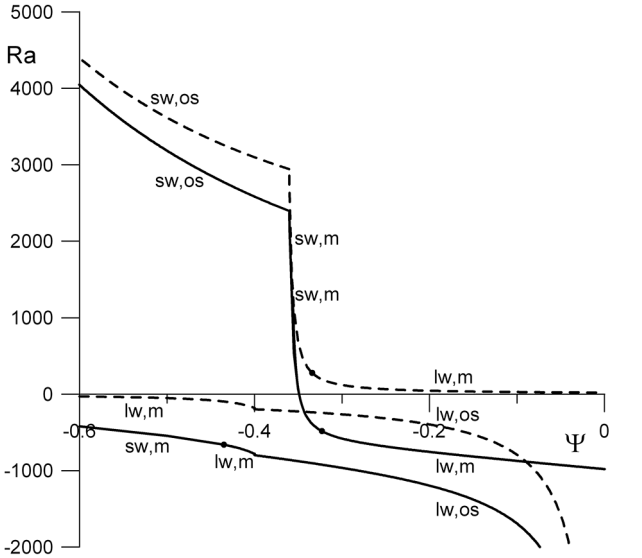

Fig. 5. Full stability map in the parameter plane Ψ-Ra for $\psi_1 = -0.4$: solid lines $\mathrm{Ra_v} = 1000$, dashed line $\mathrm{Ra_v} = 0$; notations near the boundaries are: lw, m: long-wave monotonic instability, sw, m: short-wave monotonic instability, lw, os: long-wave oscillatory instability, sw, os: short-wave oscillatory instability. The points where the instability mode changes are marked by filled circles.

fluid is illustrated by fig. 5, where the full stability map is plotted for $\mathrm{Pr} = 10$, $\mathrm{Sc_1} = 100$, $\mathrm{Sc_2} = 1000$, $\psi_1 = -0.4$.

We also analyzed the instability conditions for real ternary fluid dodecane-isobutilbensene-tetralin with equal fractions of the components. The Prandtl number for this fluid is 15.3; the transformation (6) gives the following values of the parameters: $\psi_1 = 0.109$, $\psi_2 = 0.341$ and $\mathrm{Sc_1} = 1.39 \cdot 10^3$, $\mathrm{Sc_2} = 2.24 \cdot 10^3$. As the calculations show, in the case when vibrations are absent, at these parameter values there exists a monotonic long-wave instability at heating from below and the critical value of the Rayleigh number approximately equals 12.0. Under vibrations the critical Rayleigh decreases according to the law $\mathrm{Ra} = 12.0 - 1.45\,\mathrm{Ra_v}$, thus for $\mathrm{Ra_v} > 8.28$ the instability exists not only at heating from below but also at heating from above.

6 Vibrational instability

Thus, the destabilizing effect of vibrations results in the existence of instability in zero gravity conditions (at $\mathrm{Ra} = 0$). To study this vibrational instability mode, we carried out calculations at $\mathrm{Ra} = 0$ and different values of the separation ratios. In fig. 6 the stability boundaries in the parameter plane $\Psi - \mathrm{Ra_v}$ are plotted for $\mathrm{Pr} = 10$, $\mathrm{Sc_1} = 100$, $\mathrm{Sc_2} = 1000$ at $\psi_1 = -0.4$, $\psi_1 = 0$ and $\psi_1 = 0.4$.

Let us discuss the structure of critical perturbations for the vibrational instability mode. In the first order of expansion in series of k^2, the long-wave analysis gives the following expressions for the dependences of vertical component of average velocity and average temperature on

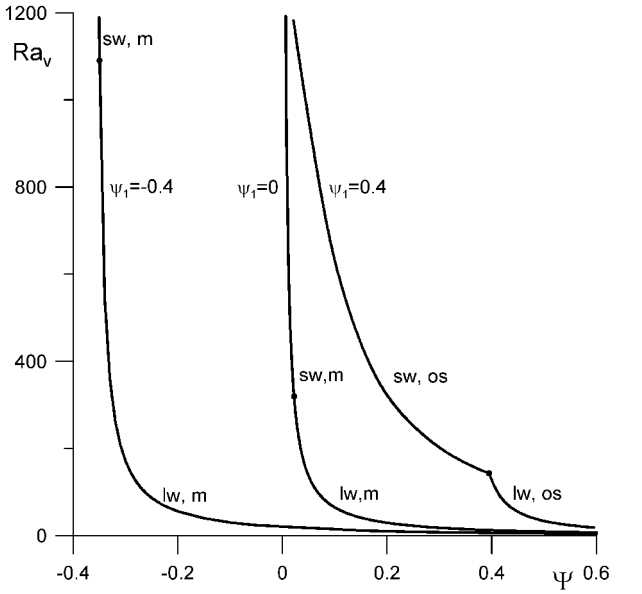

Fig. 6. The boundary of the vibrational instability ($\mathrm{Ra} = 0$) for $\psi_1 = -0.4$, $\psi_1 = 0$ and $\psi_1 = 0.4$; notations for the curves are the same as in figs. 4 and 5. The points where the instability mode changes are marked by filled circles.

vertical coordinate:

$$w_1 = \frac{\mathrm{Ra} + \mathrm{Ra_v}(1+\Psi)}{24\mathrm{Pr}}(z^4 - 2z^3 + z^2)\boldsymbol{I} \cdot \boldsymbol{\eta}_0,$$
$$\vartheta_1 = \frac{\mathrm{Ra} + \mathrm{Ra_v}(1+\Psi)}{1440}(-2z^6 + 6z^5 - 5z^4 + z)\boldsymbol{I} \cdot \boldsymbol{\eta}_0, \quad (30)$$

where $\boldsymbol{\eta}_0$ is the constant vector which corresponds to the neutral perturbations of concentrational type in zeroth order of expansion. It is seen from (30) that the dependences of w_1 and ϑ_1 on z for the vibrational instability mode are the same as that for the Soret-induced convective mode (the same conclusion is valid for concentrations).

7 Conclusions

The effect of small-amplitude high-frequency longitudinal vibrations on the stability of the horizontal layer of a ternary fluid is studied in the framework of average approach. Long-wave instability is studied analytically by the expansion into the power series with respect to wave number. It is found that, similar to the case when vibrations are absent, there exist monotonic and oscillatory long-wave instability modes. The analytical expressions are obtained for instability boundaries of both types and for the frequency of critical perturbations. The boundaries of the domains where the long-wave perturbations are most dangerous are determined in the second order of expansion. The instability to the perturbations with finite wave numbers has been studied numerically by the shooting method.

The calculations show that the vibrations leads to destabilization in the case of heating from below and to stabilization in the case of heating from above. Additionally, vibrations make influence on the parameter range where long-wave instability is most dangerous.

The critical conditions for real ternary mixture are analyzed.

New, vibrational, instability modes are found which lead to the existence of convection in zero gravity conditions.

The work was supported by Russian Scientific Foundation (grant N 14-21-00090).

References

1. P.L. Kapitsa, Sov. Phys. JETP. **21**, 588 (1951).
2. L.D. Landau, E.M. Lifshitz, *Mechanics*, Vol. **1**, 1st edition (Pergamon Press, 1960).
3. G.H. Wolf, Z. Phys. **227**, 291 (1961).
4. G.Z. Gershuni, E.M. Zhukhovitsky, Commun. AN SSSR (Doklady) **249**, 580 (1979).
5. G.Z. Gershuni, D.V. Lyubimov, *Thermal Vibrational Convection* (Wiley and Sons, 1998).
6. G.Z. Gershuni, A.K. Kolesnikov, J.C. Legros, B.I. Myznikova, J. Fluid Mech. **330**, 251 (1997).
7. G.Z. Gershuni, A.K. Kolesnikov, J.C. Legros, B.I. Myznikova, Int. J. Heat Mass Transfer **42**, 547 (1999).
8. V. Shevtsova, Y.A. Gaponenko, V. Sechenyh, D.E. Melnikov, T. Lyubimova, A. Mialdun, J. Fluid Mech. **767**, 290 (2015).
9. T.P. Lyubimova, E. Shklyaeva, J.C. Legros, V. Shevtsova, B. Roux, Adv. Space Res. **36**, 70 (2005).
10. V. Shevtsova, D. Melnikov, J.C. Legros, Y. Yan, Z. Saghir, T. Lyubimova, G. Sedelnikov, B. Roux, Phys. Fluids **19**, 017111 (2007).
11. V. Shevtsova, Adv. Space Res. **46**, 672 (2010).
12. S. Mazzoni, V. Shevtsova, A. Mialdun, D. Melnikov, Yu. Gaponenko, T. Lyubimova, Z. Saghir, Europhys. News. **41**, 14 (2010).
13. V. Shevtsova, T. Lyubimova, Z. Saghir, D. Melnikov, Y. Gaponenko, V. Sechenyh, J.C. Legros, A. Mialdun, J. Phys.: Conf. Ser. **327**, 012031 (2011).
14. V. Shevtsova, A. Mialdun, D. Melnikov, I. Ryzhkov, Y. Gaponenko, Z. Saghir, T. Lyubimova, J.C. Legros, C.R. Méc. **339**, 310 (2011).
15. I. Ryzhkov, Fluid Dyn. **48**, 477 (2013).
16. I.I. Ryzhkov, V.M. Shevtsova, Phys. Fluids **21**, 014102 (2009).
17. A.H. Nayfeh, *Introduction to Perturbation Techniques* (Wiley and Sons, 2011).
18. N.I. Lobov, D.V. Lyubimov, T.P. Lyubimova, *Solving Problems on Computer* (Perm State University, Perm, 2007).